Available online at www.sciencedirect.com
ScienceDirect
Archives of Biochemistry and Biophysics 466 (2007) 211–220
ABB
www.elsevier.com/locate/yabbi

C-terminal effect of *Thermoanaerobacter tengcongensis* ribosome recycling factor on its activity and conformation changes

Li-qiang Zhang [a,1], Hong-jie Zhang [b,*,1], Peng Guo [a], Peng Xue [b], Zhen-sheng Xie [b], Zheng Chen [a], Guo-zhong Jing [a]

[a] *National Laboratory of Biomacromolecules, Institute of Biophysics, Chinese Academy of Sciences, Beijing 100101, China*
[b] *Center for System Biology, Institute of Biophysics, Chinese Academy of Sciences, Beijing 100101, China*

Received 14 May 2007, and in revised form 22 June 2007
Available online 10 July 2007

Abstract

The *in vivo* activities and conformational changes of ribosome recycling factor from *Thermoanaerobacter tengcongensis* (*Tte*RRF) with 12 successive C-terminal deletions were compared. The results showed that *Tte*RRF mutants lacking one to four amino acid residues are inactive, those lacking five to nine are reactivated to a similar or a little higher level than wild-type *Tte*RRF, and those lacking ten to twelve are inactivated again gradually. Conformational studies indicated that only the ANS binding fluorescence change is correlated well with the RRF *in vivo* activity change, while the secondary structure and local structure at the aromatic residues are not changed significantly. Trypsin cleavage site identification and protein stability measurement suggested that mutation only induced subtle conformation change and increased flexibility of the protein. Our results indicated that the ANS-detected local conformation changes of *Tte*RRF and mutants are one verified direct reason of the *in vivo* inactivation and reactivation in *Escherichia coli*.

Keywords: C-terminal effect; Ribosome recycling factor activity; Conformational change; ANS binding fluorescence; *Thermoanaerobacter tengcongensis*; *Escherichia coli*

Protein synthesis consists of initiation, elongation, termination, and ribosome recycling. When translation of an mRNA has been completed on the ribosome, the peptidyl-tRNA with a nascent polypeptide is translocated into the ribosome P site, and a stop codon is translocated into the ribosomal A site. Then a class I release factor, RF1 or RF2, binds to the ribosomal A site, and induces the release of the nascent polypeptide. Afterwards, a class II release factor, RF3, binds to the ribosome, catalyzes the release of RF1 or RF2, and dissociates in a GTP-dependent manner [1–4], leaving behind a post-termination ribosomal complex consisting of mRNA, deacylated tRNA at the P site, and an empty A site. Dissociation of the post-termination complex, recycling of the ribosomal subunits back to a new round of initiation is an essential step in protein synthesis [5]. Ribosome recycling factor (RRF)[2] is an essential factor to trigger the dissociation of the post-termination complex [6–11]. RRF homologues have been found both in prokaryotic and eukaryotic organelles such as chloroplast and mitochondria [12–14]. All reported RRFs are highly similar in amino acid sequences [15,16]. The crystal and solution structures of RRFs from six different bacterial species have been solved [15–21]. All of these structures comprise two domains connected by a flexible hinge:

* Corresponding author. Fax: +86 10 64840672.
E-mail address: hjzhang@sun5.ibp.ac.cn (H. Zhang).
[1] These authors contributed equally to this work.

[2] *Abbreviations used:* RRF, ribosome recycling factor; EcoRRF, *Escherichia coli* RRF; TteRRF, *Thermoanaerobacter tengcongensis* RRF; TthRRF, *Thermus thermophilus* RRF; CD, circular dichroism; MS, mass spectrometry; PCR, polymerase chain reaction; IPTG, isopropyl-β-Dthiogalactopyranoside; ANS, 1-anilino-8-naphthalenesulfonate; MALDI, matrix assisted laser desorption ionization; TOF, time of flight.

0003-9861/$ - see front matter © 2007 Elsevier Inc. All rights reserved.
doi:10.1016/j.abb.2007.06.030

domain I displays a three-stranded α-helix bundle structure, and domain II exists as a three-layer β/α/β sandwich structure. The two domains are arranged in an L-shaped conformation. A study of domain swapping between *Escherichia coli* RRF (*Eco*RRF) and *Thermoanaerobacter tengcongensis* RRF (*Tte*RRF) revealed that the RRF domain I bind to ribosomes, and domain II plays a crucial role in the concerted action of RRF and EF-G for the post-termination complex dissociation [22].

Interestingly, Fujiwara et al. reported that in a cross-species-complementation experiment, the *Thermus thermophilus* RRF (*Tth*RRF) mutant lacking five amino acids from its C-terminal end (*Tth*RRFΔC5) could efficiently rescue the temperature sensitive phenotype *E. coli* strain (frr^{ts} phenotype) at the non-permission temperature of 42 °C but not the full-length protein. This suggested the existence of modulator activity of the C-terminal tail of *Tth*RRF [7,15]. Based on the crystal structure of *Tth*RRF, Toyoda et al. ascribed this modulator activity to the increase of the flexibility of the inter-domain interaction of *Tth*RRF, which was further confirmed by genetic mutation studies at the inter-domain loops [15]. Unfortunately the C-terminal modulator element was not confirmed in RRF from other bacteria species, such as *Mycobacterium tuberculosis* [23]. Therefore, it was necessary to retest the C-terminal modulator effect by using a RRF from another thermophilic bacterium.

Three questions to be addressed are particularly interesting. First, does the modulator activity of the C-terminal tail of *Tth*RRF also exist in other thermophilic RRFs? Second, if it does, how many C-terminal amino acid residues could be deleted before the activity in *E. coli* is lost? Finally, what is the structural basis of the C-terminal tail modulator activity? To answer these questions, *Tte*RRF was chosen as a model. The reasons for choosing this RRF protein were threefold. First, both *Tte*RRF and *Tth*RRF are from thermophilic bacteria, and their amino acid sequences are highly homologous [24]. Second, although neither of them can efficiently rescue *E. coli* using its frr^{ts} phenotype, slow growth of the transformant harboring plasmid for the expression of *Tte*RRF or *Tth*RRF was observed after prolonged incubation, indicating that weak residual activity still remains in *Tte*RRF and *Tth*RRF under heterologous conditions [7,24]. Twelve successive C-terminally truncated *Tte*RRF mutants (ΔC1–ΔC12) were created (Fig. 1). The ribosome recycling activity of the *Tte*RRF mutants was compared with wild-type *Tte*RRF using *in vivo* activity assays in *E. coli*. Moreover, the possible mechanism of the C-terminal tail modulator activity of thermophilic RRFs in *E. coli* was also examined by comparing subtle changes in their conformation between wild-type *Tte*RRF and its C-terminally deleted mutants by using circular dichroism (CD), fluorescence spectra, and mass spectrometry (MS).

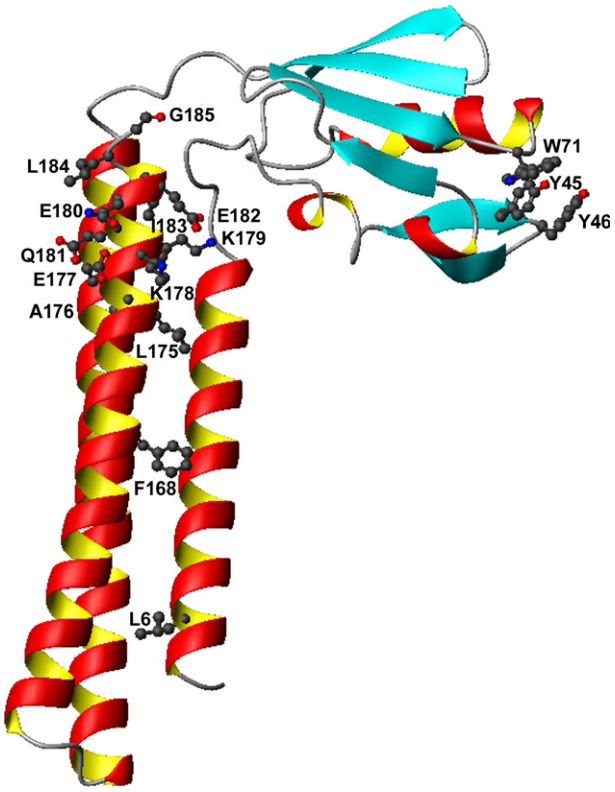

Fig. 1. Crystal structure of *Tth*RRF using PDB ID: 1EH1.pdb. *Tth*RRF is similar to *Tte*RRF in its biological features. This graph was generated using MolMol software. The side chains of eleven C-terminal residues (equivalent to twelve *Tte*RRF C-terminal residues) are indicated. The equivalent Tyr and Trp residues are also indicated as stick-and-ball figures.

Materials and methods

Bacterial strains, plasmids, and chemicals

The *E. coli* LJ14 is a MC1061 strain (frr^{ts}), in which the chromosomal wild-type *frr* allele was replaced with a mutant allele (V117D) [6], allowing *E. coli* LJ14 to grow at 30 °C but not at 42 °C. This strain was used for the *in vivo* activity assays of wild-type *Tte*RRF and its C-terminally deleted mutants by complementation analysis. pET-DB was constructed in our laboratory [25] and used for the expression of *Tte*RRF and its mutants. pQE-60, a vector with a strong T_5 promoter, was purchased from QIAGEN. It was used to construct pQE-*Tte*RRF and its C-terminally deleted mutants for analysis of the complementation of *E. coli* LJ14 (frr^{ts}). Restriction endonucleases were from NEB, and the DNA ligation kit was from Takara. All other reagents were of analytic grade.

Construction of plasmids for the expression and the in vivo complementation assay of TteRRF and its C-terminally deleted mutants

pET-DB-*Tte*RRF and pQE-*Tte*RRF were constructed as described previously [22,25]. The twelve C-terminally deleted mutants (*Tte*RRFΔC*x* ($x = 1, 2, \ldots$ and 12)) were obtained by polymerase chain reaction (PCR) using pET-DB-*Tte*RRF as a template. The N-terminal primer for all of the twelve mutants was 5′-GGT **ACC ATG G**GT AGC GAT TAT TTG AAA GAC AGT G-3′, containing an NcoI restriction site (bold). The C-terminal primers for *Tte*RRFΔC*x* ($x = 1, 2, \ldots$ and 12) were 5′-GAT **TGG ATC C**TT ATT CCA TTA TCT CCT TTT CTT TAG C-3′, 5′-GAT **TGG ATC C**TT ACA TTA TCT CCT TTT CTT TAG CCT C-3′, 5′-GAT

TGG ATC CTT ATA TCT CCT TTT CTT TAG CCT CTA C-3′, 5′-GAT **TGG ATC C**TT ACT CCT TTT CTT TAG CCT CTA C-3′, 5′-GAT **TGG ATC C**TT ACT TTT CTT TAG CCT CTA CCA TTT TG-3′, 5′-GAT **TGG ATC C**TT ATT CTT TAG CCT CTA CCA TTT TG-3′, 5′-GAT **TGG ATC C**TT ATT TAG CCT CTA CCA TTT TGT C-3′, 5′-GAT **TGG ATC C**TT AAG CCT CTA CCA TTT TGT CTA TTT CC-3′, 5′-GAT **TGG ATC C**TT ACT CTA CCA TTT TGT CTA TTT CC-3′, 5′-GAT **TGG ATC C**TT ATA CCA TTT TGT CTA TTT CCT TGA TG-3′, 5′-GAT **TGG ATC C**TT ACA TTT TGT CTA TTT CCT TGA TG-3′, 5′-GAT **TGG ATC C**TT ATT TGT CTA TTT CCT TGA TGT ATT TA-3′, respectively, containing BamHI restriction sites (bold). The PCR products were inserted into the NcoI and BamHI sites of pET-DB and pQE60, respectively, after digestion with the same enzymes, resulting in pET-DB-*Tte*RRFΔC*x* and pQE-*Tte*RRFΔC*x*. Each plasmid (pET-DB-*Tte*RRF and pET-DB-*Tte*RRFΔC*x*) was transformed into *E. coli* BL21(DE3)pLysS for the expression of *Tte*RRF and its mutants and each plasmid (pQE-*Tte*RRF and pQE-*Tte*RRFΔC*x*) was transformed into the *E. coli* LJ14 strain (frr^{ts}) for the complementation assay.

Expression and purification of TteRRF and its C-terminally deleted mutants

All *Tte*RRF proteins were expressed in a soluble form and the details of the purification and characterization of the proteins were as described previously [24,26]. In brief, each plasmid was transformed into *E. coli* BL21(DE3)pLysS cells. Fresh cultures of the transformants were induced with 0.5 mM isopropyl-β-D-thiogalactopyranoside (IPTG), and the over-expressed proteins were purified by metal chelating affinity chromatography. Because twenty-two amino acid residues including a His_6 tag and a thrombin cleavage site were fused in-frame to the N-terminal end of each protein when its gene was cloned into the pET-DB vector [25], each protein was first expressed as a His_6-tagged protein. Further purification was performed using a Sephacryl S100 column after the N-terminal peptide had been removed by thrombin cleavage. Each purified protein appeared as a single band on an SDS 15% polyacrylamide gel. The protein concentration was determined using the same molar extinction coefficient of 10810 M^{-1} cm^{-1} at 280 nm, which was calculated from the amino acid compositions following the procedure described by Pace et al. [27].

Circular dichroism (CD) spectra

The CD spectra of *Tte*RRF and selected *Tte*RRFΔC*x* mutants ($x = 1$, 4, 5, 9, 12) were obtained at 25 °C using an Applied Photophysics PiStar-180 spectrometer with a 1-mm path length quartz cuvette. The protein concentration in the samples was 5 μM for far-UV CD (250–200 nm) in 50 mM phosphate buffer, pH 7.4. The CD spectra data were taken at 1-nm intervals with an integration time of 1 s. The data represent the average of five scans after correction for the buffer baseline and were reported as mean residue ellipticity ([θ]).

In vivo assays for RRF activity

The *in vivo* assay was performed by monitoring the complementation of *E. coli* LJ14 (frr^{ts}) with *Tte*RRF and its mutants (*Tte*RRFΔC*x*s), respectively. The plasmids pQE-*Tte*RRF or pQE-*Tte*RRFΔC*x*s, which express *Tte*RRF or the *Tte*RRFΔC*x* mutants, were transformed into *E. coli* LJ14 (frr^{ts}). Since the wild-type *Tte*RRF has weak complementation of *E. coli* LJ14 (frr^{ts}), in order to easily observe the changes in complementation activity, cultures were started with 2% (v/v) inoculums from freshly grown (at 30 °C) overnight cultures instead of 0.06% (v/v) as described previously [22]. The growth was monitored by recording culture turbidities at 600 nm at regular intervals at the permissive (30 °C) or non-permissive (42 °C) temperatures.

Fluorescence spectra

The intrinsic fluorescence emission spectra of *Tte*RRF and selected *Tte*RRFΔC*x* mutants ($x = 1$, 4, 5, 9, 12) were measured at 25 °C using a Hitachi F-4500 fluorescence spectrophotometer with a slit width of 5 nm. The excitation wavelengths were 284 nm and the concentration of each protein was 5 μM in 50 mM phosphate buffer, pH 7.4. For measurement of binding fluorescence, 1-anilino-8-naphthalenesulfonate (ANS, Sigma) was used as a hydrophobic fluorescence probe. The excitation wavelength was 350 nm, and each sample contained 5 μM RRF protein and 50 μM ANS in 50 mM phosphate buffer, pH 7.4.

GdnHCl-induced equilibrium denaturation

To investigate the changes in stability induced by the C-terminal deletions, the *Tte*RRFΔC*x* mutants ($x = 1$, 4, 5, 9, 12) were selected according to their *in vivo* complementation activity to *E. coli* LJ14 (frr^{ts}). GdnHCl-induced denaturation of *Tte*RRF and its selected mutants was measured at 25 °C by monitoring the change in the CD signal $[\theta]_{222\,nm}$ with a 1-mm path length quartz cuvette. Each sample contained 5 μM of protein in 50 mM phosphate buffer, pH 7.4, with different concentrations of GdnHCl. The samples were incubated overnight at 25 °C before the experiments were conducted. The data were obtained by the average of four scans. The unfolding progress was determined by

$$f = \frac{y - y_N}{y_D - y_N}, \tag{1}$$

where y is the measured CD, y_N is the CD for the native state of RRF and y_D is that of the extrapolated value for the denatured state, assuming that they are linearly dependent on the GdnHCl concentration, i.e.,

$$y_N = y_N^0 + m_N[\text{GdnHCl}], \tag{2}$$

and

$$y_D = y_D^0 + m_D[\text{GdnHCl}]. \tag{3}$$

Evaluation of the isothermal unfolding curves was performed numerically following the procedure of Santoro and Bolen [28] using two-state model equations through the software of SigmaPlot 6.0:

$$f = \frac{y_N + y_D Q}{1 + Q}, \tag{4}$$

$$Q = \exp\left(-\frac{\Delta G_D^0(H_2O) - m_G[\text{GdnHCl}]}{RT}\right), \tag{5}$$

where $\Delta G_D^0(H_2O)$ is the standard Gibbs free energy change for unfolding in the absence of denaturant, and m_G is the slope of the plot of ΔG_{app}^0 versus denaturant concentration, according to:

$$\Delta G = \Delta G_D^0(H_2O) - m_G[\text{GdnHCl}]. \tag{6}$$

Limited hydrolysis of protein samples using trypsin and peptide identification by MALDI-TOF-MS

*Tte*RRF and selected mutants *Tte*RRFΔC*x*s ($x = 1$, 4, 5, 9, and 12) were dissolved with a concentration of 1 mg/ml in the cleavage buffer (100 mM Tris–HCl, 2 mM $CaCl_2$ at pH 7.5), then trypsin (from Sigma, Ca. No. T 1426) was added with a final concentration of 1 μg/ml and incubated at 37 °C for different lengths of time. The samples were first precipitated by adding cold trichloric acetic acid to a final concentration of 10% and incubated on ice for 30 min, then collected by centrifugation at 13,000*g* at 4 °C for 20 min. The pellets were then lyophilized. Before mass spectrum measurement, the dried samples were first dissolved in 10 μl solution containing 50% MeCN and 0.1% trifluoric acetic acid for matrix assisted laser desorption ionization-time of flight-mass spectrometry (MALDI-TOF-MS) analysis [29]. A solution of freshly prepared α-cyano-4-hydroxycinnamic acid (10 mg/ml) in 70% MeCN and 0.1% TFA was mixed with the same volume of the above sample solution. A total of 1.0 μl of the sample mixture was applied onto the MALDI target and allowed to dry. MALDI-TOF-MS were acquired on an AXIMA-CFP plus mass spectrometer equipped with a 337.1-nm nitrogen laser. Mass spectra were obtained in positive ion and linear mode with an acceleration voltage of 20 kV and averaged over 100 laser shots. Each spectrum was internally

calibrated using single charged and double charged apomyoglobin (equine) as standard. The data above 3000 Da was collected and analyzed using Masslynx v4.0 software.

Results

In vivo complementation activity assays of TteRRF and its C-terminally deleted mutants in E. coli LJ14 (frr^{ts})

It is known that RRF is an essential protein for bacterial growth since deletion of the RRF gene is lethal in *E. coli* [30], as are temperature-sensitive (frr^{ts}) mutations [6]. Complementation analysis allowed the *in vivo* activity to be tested. The *Tte*RRF and its C-terminally deleted mutants' genes cloned in pQE-*Tte*RRF and pQE-*Tte*RRFΔC*x*s were tested for intergenetic complementation of the *E. coli* LJ14 (frr^{ts}) strain. The growth rates of the various transformants in liquid cultures at the permissive (30 °C) and non-permissive (42 °C) temperatures were monitored. As expected, all the transformants harboring pQE-*Tte*RRF or pQE-*Tte*RRFΔC*x*s grew at the same rate at the permissive temperature (Fig. 2a), suggesting that the expression of these RRFs was not toxic to *E. coli* (data not shown) [22]. However, at the non-permissive temperature (42 °C), the growth of all of the transformants was inhibited to different degrees (Fig. 2b). For Wt *Tte*RRF, even after 12 h culture, no exponential growth phase occurred, which was consistent with our previous report [24]. In order to compare the relative activity change of *Tte*RRF mutants, Fig. 2c shows the relative growth rate of *E. coli* LJ14 (frr^{ts}) transformed with pQE-*Tte*RRF or pQE-*Tte*RRFΔC*x*s ($x = 1, 2, \ldots$ and 12) at the non-permissive temperature (42 °C) after 8 h culture. It can be seen that deletion of one to four residues from the C-terminal end of *Tte*RRF (*Tte*RRFΔC1–*Tte*RRFΔC4) causes the growth rate to be severely decreased; deletion of five to nine residues (*Tte*RRFΔC5–*Tte*RRFΔC9) causes the growth rate to be increased to the same level or even a little higher than the wild-type *Tte*RRF; however, further deletion of up to twelve residues results in a gradual but complete loss of growth. These results indicated that C-terminal residues of *Tte*RRF could modulate its complementary activity in *E. coli*.

Far-UV CD spectra of TteRRF and its C-terminally deleted mutants

Far-UV CD spectra were used to assess the secondary structure, and in particular, the α-helix content of *Tte*RRF

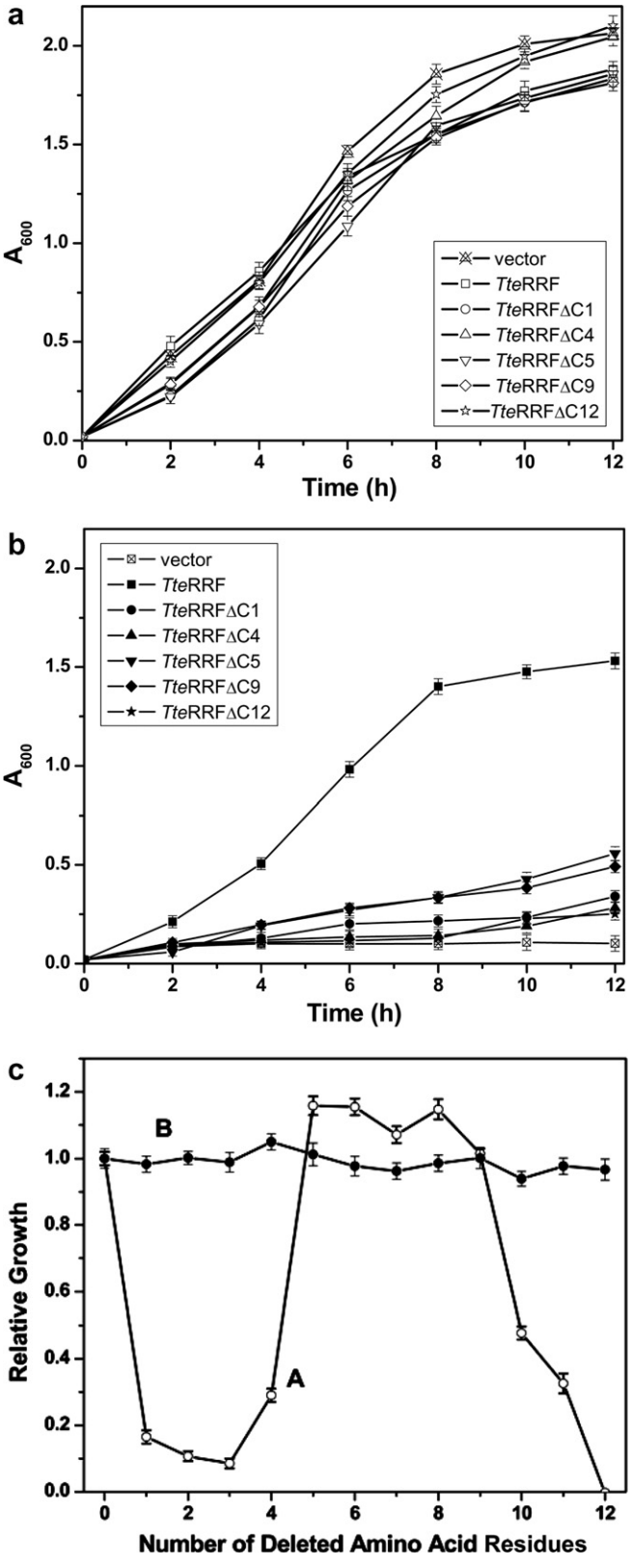

Fig. 2. *In vivo* activity assays of *Tte*RRF and its C-terminal mutants at different temperatures. (a) Growth curves of various transformants of *E. coli* LJ14 (frr^{ts}) at the permissive temperature (30 °C). Vector, transformants with pQE60, *Tte*RRF, transformants with pQE-*Tte*RRF, *Tte*RRFΔC*x* ($x = 1, 4, 5, 9, 12$), transformants with pQE60-*Tte*RRFΔC*x* mutants ($x = 1, 4, 5, 9, 12$). (b) Growth curves of various transformants of *E. coli* LJ14 (frr^{ts}) at the non-permissive temperature (42 °C). The transformants are the same as those indicated in (a). (c) Relative growth rate of *E. coli* LJ14 (frr^{ts}) transformed with pQE-*Tte*RRF or pQE-*Tte*RRFΔC*x* mutants ($x = 1, 2, \ldots 12$) at the non-permissive temperature (42 °C). The bacterial culture turbidity was monitored at 600 nm after incubation for 8 h, and the relative value of transformant harboring pQE-*Tte*RRF was set as unity. The details of the experiment conditions are described in the text.

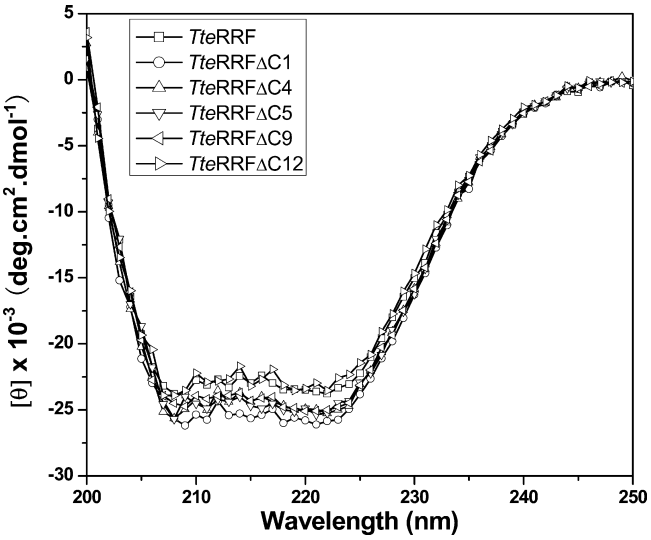

Fig. 3. Far-UV CD spectra of *Tte*RRF and its C-terminally deleted mutants *Tte*RRFΔC1, *Tte*RRFΔC4, *Tte*RRFΔC5, *Tte*RRFΔC9, and *Tte*RRFΔC12. The spectra were obtained at 25 °C; the details of the experimental conditions are described in the text.

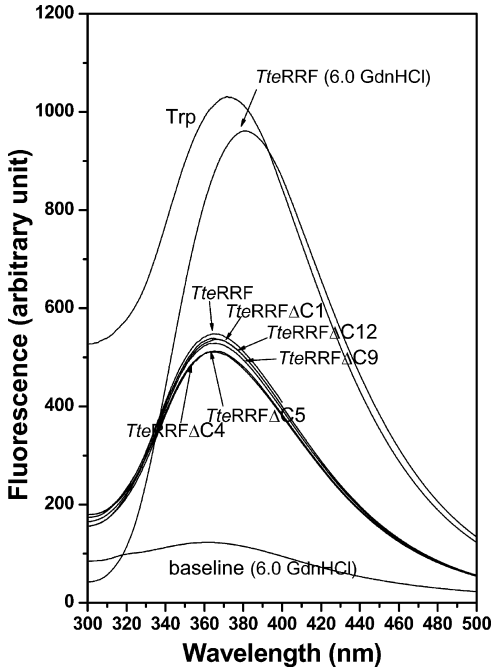

Fig. 4. Intrinsic fluorescence spectra of *Tte*RRF and its C-terminally deleted mutants. Intrinsic fluorescence emission spectra of *Tte*RRF and its mutants *Tte*RRFΔC1, *Tte*RRFΔC4, *Tte*RRFΔC5, *Tte*RRFΔC9, and *Tte*RRFΔC12 at 25 °C. The concentration of each protein was 5 μM in 50 mM phosphate buffer, pH 7.4. *Tte*RRF (6.0 GdnHCl) denotes the spectra measured under 6M GdnHCl, and Gly-Trp denotes the spectrum of dipeptide with a concentration of 5 μM. The baseline denotes only 6 M GdnHCl in the buffer. The excitation wavelength was 284 nm and the emission wavelength was from 300 nm to 500 nm. The slits of both the excitation and emission were 5 nm.

and its mutants. The appearance of two negative peaks at 208 and 222 nm in a CD spectrum is usually considered to be indicative of the content of α-helical structure in a protein [31,32]. The helix fraction can be calculated based on the mean residual ellipticity of a protein at 222 nm according to the following equation [33,34]:

$$\text{Helix}\% = -[\theta]_{222\text{nm}} \cdot n/40,000 \cdot (n-4),$$

where n is the number of peptide bonds. Fig. 3 shows the far-UV CD spectra of *Tte*RRF and its mutants. Deletion of one residue from the C-terminal end of *Tte*RRF leads to the signal at 222 nm increasing about 8%, but the deletions of four or five residues leads to a signal increase of about 4%. Even for *Tte*RRFΔC12, the signal decrease at 222 nm was only 8%. These results indicate that deletion of the C-terminal residues may have no significant effect on the secondary structure of *Tte*RRF, especially the α-helix structure of *Tte*RRF domain I, which corresponds well with the finding the activity of some C-terminally deleted mutants was equal to or even higher than the activity of the wild-type *Tte*RRF in *E. coli*.

Intrinsic fluorescence spectra of TteRRF and its C-terminally deleted mutants

In RRF molecules, there are four tyrosine residues and one tryptophan residue in the RRF molecule located at positions 4 and 166 (Y_4 and Y_{166}) in domain I, and at positions 43, 44, and 69 (Y_{43}, Y_{44}, and W_{69}) in domain II of *Tte*RRF [24]. Changes in the intrinsic fluorescence spectra after excitation at 284 nm could reflect the changes in the local environment of these aromatic residues. Fig. 4 shows the fluorescence emission spectra of *Tte*RRF and its mutants. Compared with the fluorescence emission spectrum of *Tte*RRF in 6 M GdnHCl, the intrinsic fluorescence intensity of both *Tte*RRF and its mutants is much lower, showing that the intrinsic fluorescence for both *Tte*RRF and its mutants is quenched by an intramolecular mechanism that has not been identified yet [35]. There was only a slight difference in their fluorescence emission spectra, indicating that the C-terminal deletions did not significantly change the local environment of these aromatic residues (domains I and II) in the mutants.

ANS binding fluorescence spectra of TteRRF and its C-terminally deleted mutants

ANS is widely used as a hydrophobic fluorescence probe to measure the changes in the surface hydrophobicity of proteins. The difference in surface hydrophobicity reflects changes in the exposure of hydrophobic side chains, which could be used as an indicator of the local conformation change of hydrophobic areas [36–40]. To further examine the possible changes in the conformation induced by the C-terminal deletions of *Tte*RRF, the ANS binding fluorescence spectra of *Tte*RRF and its mutants were measured. Fig. 5a shows the fluorescence emission spectra of ANS in the presence of *Tte*RRF and its mutants. In contrast to ANS itself, wild-type *Tte*RRF could bind with ANS,

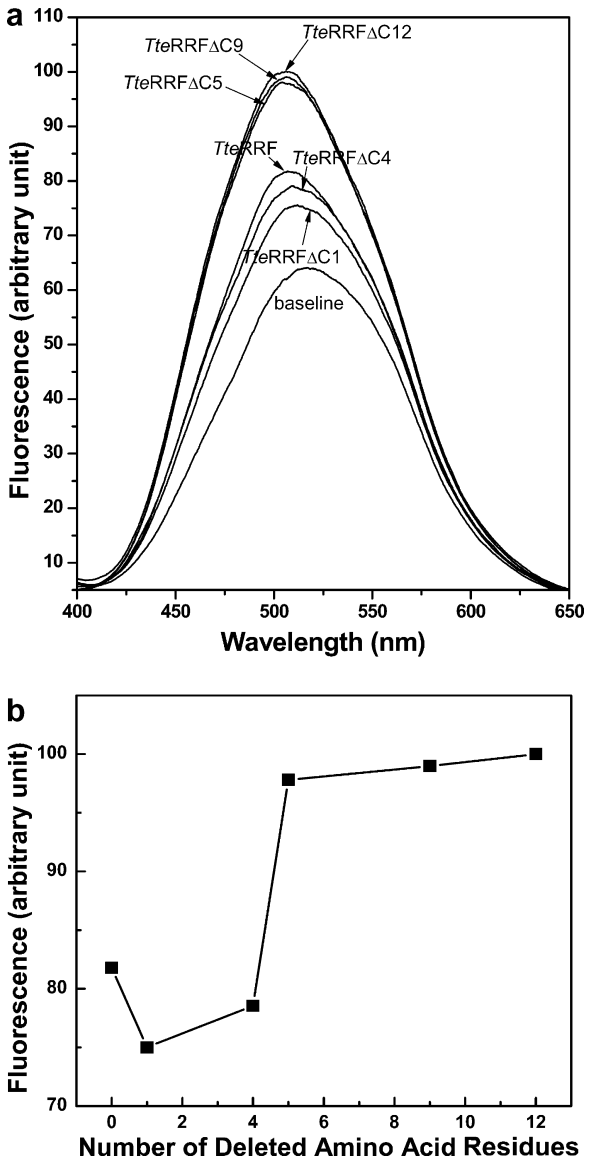

Fig. 5. ANS-binding fluorescence spectra of *Tte*RRF and its C-terminally deleted mutants. (a) Fluorescence spectra of ANS in the presence of *Tte*RRF and its C-terminal mutants *Tte*RRFΔC1, *Tte*RRFΔC4, *Tte*RRFΔC5, *Tte*RRFΔC9, and *Tte*RRFΔC12 at 25 °C. The excitation wavelength was 350 nm, and each sample contained 5 μM RRF protein and 50 μl ANS in 50 mM phosphate buffer, pH 7.4. (b) The fluorescence intensity change versus the number of deleted C-terminal residues at 507 nm. The data were obtained from (a).

as indicated by the emission maximum wavelength movement from 520 to 507 nm, and the fluorescence intensity increase, suggesting that the molecular surface of *Tte*RRF has one hydrophobic area, suitable for transferring ANS from aqueous solution to a hydrophobic microenvironment in certain degree. C-terminal deletion of *Tte*RRF could lead to changes in the ANS binding fluorescence spectrum. For *Tte*RRFΔC1 and *Tte*RRFΔC4, the ANS binding fluorescence intensity became weaker than wild-type *Tte*RRF with a small but detectable red shift to 511 nm at its maximum emission wavelength, but for *Tte*RRFΔC5, *Tte*RRFΔC9 and *Tte*RRFΔC12, the ANS binding fluorescence intensities increased obviously, with a small blue shift to 505 nm, in contrast to wild-type *Tte*RRF. The fluorescence intensity change at 507 nm, the emission maximum wavelength for wild-type *Tte*RRF, was plotted versus the number of residues deleted as shown in Fig 5b. This plot shows clearly the ANS binding fluorescence intensity change of *Tte*RRF induced by C-terminal deletion, suggesting that the C-terminal deletions make the local conformation of the hydrophobic areas of *Tte*RRF mutants change from a suitable sorting conformation of ANS for wild-type *Tte*RRF to less suitable sorting conformations for *Tte*RRFΔC1 and ΔC4, and then to much suitable sorting conformations for *Tte*RRFΔC5, ΔC9, and ΔC12.

MALDI-TOF-MS analysis of TteRRF and its C-terminally deleted mutants after limited proteolysis with trypsin

Mass spectrometry has been used to determine protease cleavage sites, serving as a powerful tool to probe subtle conformational changes induced by mutations [29]. In order to obtain more information about subtle conformation changes, *Tte*RRF and its mutants, *Tte*RRFΔC1, ΔC4, ΔC5, ΔC9, and ΔC12, were analyzed by MALDI-TOF-MS after trypsin digestion as described in Materials and methods. Fig. 6 shows the mass spectra of *Tte*RRF and its mutants after digestion for 5 min, which represents the digestion at an early stage. For *Tte*RRF, there are only three peaks of this protein with one, two, and three hydrogen ions bonded, indicating that no obvious protease cleavage occurred under the selected conditions. In contrast, for *Tte*RRFΔC1, ΔC4, and ΔC5, besides the multiple charged molecular peaks of these intact proteins, a number of additional peaks were observed, and the peak number increased from *Tte*RRFΔC1 to ΔC4, and to ΔC5. However, with further deletion for *Tte*RRFΔC9 and ΔC12, the additional peaks shown above became significantly decreased, indicating that the conformational integrity of *Tte*RRFΔC9 and ΔC12 was severely damaged, causing them to be much more sensitive to proteolysis. The partially digested products were degraded into small peptides under the same conditions; these peptides could not be identified when the mass range was above 3000 Da selected. Table 1 lists some of the identified peptides of *Tte*RRFΔC1 from Fig. 6 with abundant peaks. It can be seen that most of them are secondary cleavage products, and they were distributed in domains I and II and the hinge regions. Although no initial enzyme cleavage site could confidently be determined from the identified peptides, these cleavage sites became more accessible to trypsin than the intact *Tte*RRF molecule, suggesting that the C-terminally deleted mutations induce some conformation changes around these cleavage sites, which makes these cleavage sites more flexible and easy for protease access. In other words, the C-terminal truncation of *Tte*RRF induced subtle conformational change, including flexibility change.

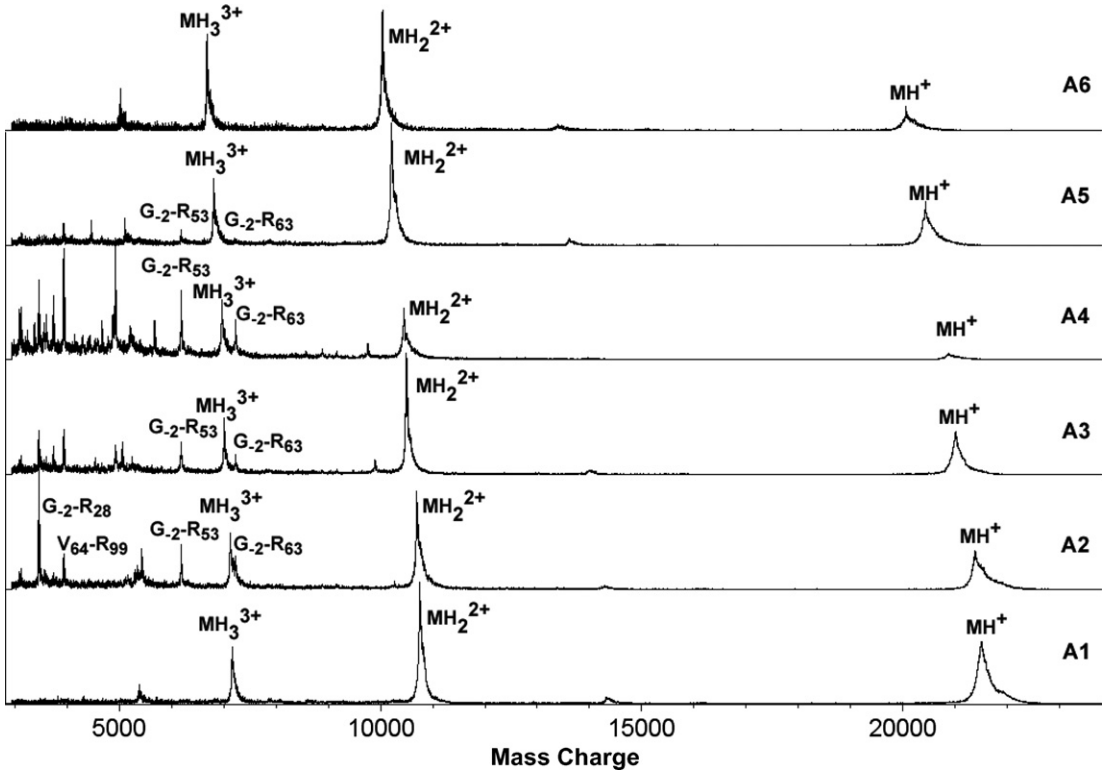

Fig. 6. MALDI-TOF-MS analysis of *Tte*RRF and its C-terminally deleted mutants after limited proteolysis with trypsin. MALDI-TOF-MS of *Tte*RRF and its mutants digested with trypsin at 5 min. (A1) MS for wild-type *Tte*RRF. (A2) MS for *Tte*RRFΔC1. (A3) MS for *Tte*RRFΔC4. (A4) MS for *Tte*RRFΔC5. (A5) MS for *Tte*RRFΔC9. (A6) MS for *Tte*RRFΔC12. The molecular ion peaks identified were labeled as MH^+, MH_2^{2+}, and MH_3^{3+} for one, two and three charges. In addition to the molecular ion peaks, some digested peptides were also labeled out.

Table 1
Trypsin hydrolyzed peptide identification of *Tte*RRFΔC1

Peptide sequence	Theoretical value of peptide	Measured value $MH^+(m/z)$ (+deviation)	Cleavage site position
MH^+	21391.51	21401.4(+9.89)	None
MH_2^{2+}	21391.51	10698.8(+2.045)	None
MH_3^{3+}	21391.51	7132.13(+0.63)	None
A_{29}–E_{184}	17953.7	17947.6(−7.1)	Close to hinge
V_{64}–E_{184}	14188.40	14186.6(−2.80)	Domain II
R_{110}–E_{184}	9088.9	9085.6(−4.3)	Domain I
A_{29}–R_{109}	8888.23	8889.3(+0.07)	Hinge
G_{-2}–R_{63}	7234.27	7235.8(+0.53)	Domain II
G_{-2}–R_{53}	6184.07	6183.5(−1.57)	Domain II
D_{134}–E_{184}	6185.02	6183.5(−2.52)	Domain I
D_{134}–K_{178}	5425.14	5429.8(+3.66)	Domain I
K_{141}–E_{184}	5429.19	5429.8(−1.39)	Domain I
A_{32}–K_{80}	5431.24	5429.8(−3.44)	Hinge and domain II
V_{97}–R_{129}	3922.72	3928.4(+5.68)	Domain II and domain I
V_{64}–R_{99}	3931.55	3928.4(−4.15)	Domain II
G_{-2}–R_{28}	3455.78	3457.9(+1.12)	Close to hinge

Stability of TteRRF and its C-terminally deleted mutants

Thermal unfolding of *Tte*RRF has been reported previously [24]. Within a temperature range up to 85 °C, no unfolding occurs. Among the selected mutants in this study, unfolding of only *Tte*RRFΔC12 could be completed at temperatures below 85 °C, by a two-state mechanism (data not shown), suggesting that all of the truncation mutants used could be folded with similar but not the same structures as WT *Tte*RRF, including at the *in vivo* complementary activity assay temperature of 42 °C. In order to quantitatively evaluate the stability changes induced by the C-terminal deletions, GdnHCl-induced isothermal unfolding of *Tte*RRF and its selected mutants, *Tte*RRFΔC1, ΔC4, ΔC5, ΔC9, and ΔC12, were measured by monitoring the changes of the far-UV CD signal at 222 nm. Fig. 7a shows the equilibrium unfolding transition progress in a series of GdnHCl concentrations, where the native states were set as zero and the fully unfolded states at 6 M GdnHCl were set as unity. The unfolding of each RRF follows a two-state transition, and the thermodynamic parameters of the standard Gibbs free energy ($\Delta G^0_{H_2O}$) and m_G values, the slope of free energy versus denaturant concentrations, were obtained by numerically fitting the data to Eqs. (1)–(6). The C_m value, the concentration of GdnHCl at which half of each protein molecule is denatured, was also calculated from Eq. (6) (Table 2). The deletion of C-terminal residues leads to protein stability determined by C_m value decreased monotonically, while according to the Gibbs free energy values, the stability of *Tte*RRF was less changed until nine residues from its C-terminal was deleted. Further deletion of the C-terminal

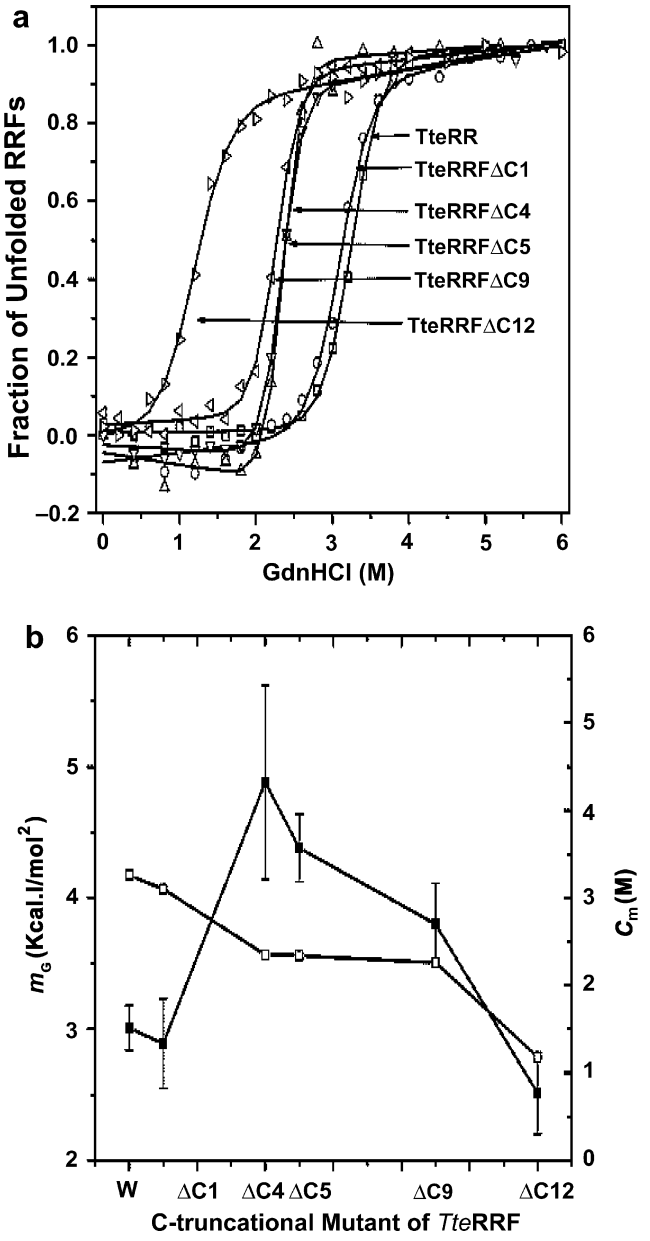

Fig. 7. GdnHCl-induced isothermal unfolding of *Tte*RRF and its selected mutants. (a) Unfolding progress of *Tte*RRF and its mutants monitored by changes in the CD signal at 222 nm at 25 °C. Squares (□) indicate *Tte*RRF, circles (○) *Tte*RRFΔC1, upright triangle (Δ) *Tte*RRFΔC4, upside down triangle (▽) *Tte*RRFΔC5, triangle pointing left (◁) *Tte*RRFΔC9 and triangle pointing right (▷) *Tte*RRFΔC12. (b) The relationship of m_G and C_m values versus the number of residues deleted at the *Tte*RRF C-terminal. The filled circles (●) denote the m_G value changes and open circles (○) the C_m changes. Detailed experimental conditions are described in Materials and methods.

residues causes the *Tte*RRF to become less stable, as indicated by both Gibbs free energy and the C_m values. The different changes of Gibbs free energy and C_m values for *Tte*RRF and its mutants are due to the m_G value changes [Eq. (6)]. As shown in Fig. 7b, the deletion of four C-terminal residues leads to a significant increase of the m_G value from 3.01 to 4.88 kcal l/mol^2 (62% increase), but the deletion of five to twelve C-terminal residues leads to a gradual decrease of their m_G values. As the denaturant m_G value has been linear correlated well with the change of solvent accessible surface areas of denatured and native proteins [42], and deletion of the C-terminal residues decreases only slightly the solvent accessible surface area of the unfolded *Tte*RRF, these m_G changes could be used as an indicator for native protein surface change caused by C-terminal mutation. This result supports the hydrophobic surface change of *Tte*RRF mutants detected by ANS analysis.

Table 2
Stability parameters from isothermal GdnHCl-induced unfolding

Proteins	ΔG^0_{H2O} (kcal/mol)	m_G (kcal l/mol^2)	C_m (M)
Wt *Tte*RRF	9.83 ± 0.56	3.01 ± 0.17	3.26
*Tte*RRFΔC1	8.95 ± 1.10	2.89 ± 0.34	3.10
*Tte*RRFΔC4	11.48 ± 1.74	4.88 ± 0.74	2.35
*Tte*RRFΔC5	10.25 ± 0.61	4.38 ± 0.26	2.34
*Tte*RRFΔC9	8.59 ± 0.72	3.80 ± 0.31	2.26
*Tte*RRFΔC12	2.97 ± 0.49	2.51 ± 0.31	1.18

Discussion

In the present study, it was verified that the C-terminal of *Tte*RRF, a highly homogenous thermophilic protein, functions similar to *Tth*RRF in *E. coli*. Removing one amino residue from its C-terminal leads to *Tte*RRF inactivation. Removing five residues is helpful for expressing its dissociation function in *E. coli*, and the maximal number of residues that could modulate *Tte*RRF's activity is twelve. This result confirmed the hypothesis that C-terminal residues serve as a modulator element for the functional expression of RRF. The difference in the regulation behavior of *Tte*RRF and *Tth*RRF is that after deletion of five residues at its C-terminal, *Tth*RRF could obtain much higher dissociation activity than wild-type *Tth*RRF in *E. coli* [7], while for *Tte*RRF the degree of activation is restored to values only equal to or a little higher than wild-type *Tte*RRF. If a low inoculation dose of 0.06% is used (as most laboratories used), even after 12 h culture, the *E. coli* LJ14 strain has no significant growth (data not shown), and the reactivation effect modulated by its C-terminal cannot be observed. This difference indicated that the role of C-terminal modulation for *Tth*RRF and *Tte*RRF is slightly different. The deletion of ten to twelve C-terminal residues causes *Tte*RRF to lose its dissociation activity gradually as its stability becomes significantly lower and it becomes more susceptible to protease digestion (Figs. 6 and 7).

Conformational studies of *Tte*RRF mutants indicated that successive deletion of the twelve C-terminal residues induced a local conformation change detected by extrinsic fluorescence ANS probe. The fluorescence intensity of ANS is sensitive to dielectric properties of its environment and is enhanced under hydrophobic conditions. Wild-type *Tte*RRF could bind one ANS (data not shown) with an increase in the fluorescence emission intensity and a blue

shift of the emission maximum wavelength, indicating that *Tte*RRF has a hydrophobic surface area at its molecular surface, defining a meaningful local conformation. Truncation mutants of *Tte*RRFΔC1 and *Tte*RRFΔC4 lead to the decreased binding fluorescence of *Tte*RRF to ANS (Fig. 5b), indicating the interaction surface of *Tte*RRF with ANS has been changed. This decrease coincides with the inactivation of the weak *Tte*RRF complementary activity in *E. coli* (Fig. 2c). When five residues from its C-terminal were removed, the ANS binding fluorescence was increased to a level higher than that of wild-type *Tte*RRF (Fig. 5b), and the residue activity of *Tte*RRF mutants was observed to be as high as or a little higher than wild-type *Tte*RRF (Fig. 2c). Further deletion of *Tte*RRF C-terminal residues caused the ANS binding fluorescence to remain at a similar level. Correspondingly, the complementary activity of *Tte*RRF mutants retained its activity from *Tte*RRFΔC5 to *Tte*RRFΔC9, and then the activity decreased gradually. The gradually decreased activity from *Tte*RRFΔC10 to *Tte*RRFΔC12 was due to a decrease in the protein stability, causing the proteins to be more accessible to protease, in other words, causing subtle conformation changes of *Tte*RRF. The same trends of ANS binding fluorescence with *Tte*RRF complementary activity from *Tte*RRFΔC1 to ΔC9 in *E. coli* suggest a direct correlation between the local conformational change of the ANS binding hydrophobic surface and *Tte*RRF complementary activity in *E. coli*. In contrast, no significant globule conformation change is indicated by the similar far-UV CD spectra (Fig. 3), especially the α-helix structure of *Tte*RRF domain I, and local conformational changes at the aromatic residues by similar intrinsic fluorescence (Fig. 4). At present the location of the ANS binding site on *Tte*RRF is unclear. However, structural analysis implies the interdomain region of RRF is one possible target. The main function of domain I in RRF is to bind with ribosome 70S complex, and domain II mainly has a disassembly function through concerted interaction with EF-G. This molecule could regulate its interdomain location by changing the interdomain angle, while keeping each domain conformation unchanged, as suggested by the crystal structure of *E. coli* RRF with a hydrophobic ligand decyl-β-D-maltopyranoside (PDB ID: 1EK8) or without this ligand (PDB ID: 1ISE) [18,19], of which each domain showed small RMSD. Moreover, previous study also suggests that there is a hydrophobic hole at the interdomain region, which could be targeted by a decyl-β-D-maltopyranoside hydrophobic side chain. Although the C-terminal of domain I has no direct strong interaction with domain II, interdomain interaction has been found from several RRF crystal structure (e.g., in *Tm*RRF crystal structure, there is electrostatic interaction between Lys31NE close to domain I and Glu181OE2 at domain II with a distance of 3.08 Å [17] but not in *Tth*RRF crystal structure [20].) This interaction tends to decrease the interdomain angle, and deletion of the C-terminal residues is helpful for this change. However, when five residues were deleted, the above interdomain interaction was removed and caused the interdomain angle increase. The trend of the structural change analysis was the same as observed from the ANS binding fluorescence change and *in vivo* complementary activity changes. This strongly implies that the interdomain region may be a potential ANS binding region.

Previous studies by Toyoda *et al*. assumed that the flexibility increase of the interdomain loops is the dominant reason of *Tth*RRF reactivation in *E. coli* [20]. However, none of the conformation probes used in this study could be used as specific probes for the interdomain flexibility change in solution. Hence, at present it is unclear whether C-terminal truncation of *Tte*RRF could specifically increase the flexibility of the interdomain hinge. In contrast, it is clear that C-terminal truncation of *Tte*RRF could increase molecular flexibility as a whole. According to the C_m values of *Tte*RRF and its mutants, the C-terminal deletions cause the mutants to be unstable to different extents, depending on the number of amino acid residues deleted. Since a protein's flexibility correlates well with its stability (e.g., overall flexibility is reduced when thermostability is increased [41]), the fact that *Tte*RRF mutants lack five to nine amino acid residues from their C-terminal end (*Tte*RRFΔC5 to ΔC9) and have enhanced their complementation activity to the temperature-sensitive *E. coli* strain (frr^{ts}) at the non-permissive temperature (42 °C) may be due to the fact that the mutations provide these mutants with more suitable flexibility to interact with ribosome 70S and *Eco*EF-G; excessive flexibility for ΔC12 causes the loss of their complementation activity. However, the overall flexibility change itself was not responsible for the inactivation of *Tte*RRFΔCx ($x = 1, 2, 3, 4$) versus the wild-type of *Tte*RRF, indicating that the flexibility increase may contribute to but is not the sole reason for *Tte*RRFΔCx ($x = 1, 2, \ldots 9$) activity change. This is further confirmed by the trypsin digestion experiments. That results indicated that even for mutant *Tte*RRFΔC1 the flexibility increase as suggested by trypsin cleavage site increase is not limited only in the interdomain region, but is also located at domains I and II. This conformation change can regulate the inactivation or reactivation of the *in vivo* complementary activity of *Tte*RRF through its C-terminal tail.

In summary, in this report the modulator role of the *Tte*RRF C-terminus on its complementary activity in *E. coli* was verified by using a successive deletion mutation. Removing one to four residues could inactivate *Tte*RRF's complementary activity and removing five to nine residues could reactivate *Tte*RRF's complementary activity in *E. coli*. The structural basis of this modulating effect is due to local conformational changes as monitored by ANS fluorescence probe. Although the role of flexibility increase of the interdomain hinge in the reactivation of *Tte*RRF could not be ruled out, it is clear that C-terminal truncation inducing a flexibility increase is not limited only in the inter-domain loops, but is also located at domains I and II.

Acknowledgments

We thank Professor A. Kaji, Department of Microbiology, School of Medicine, University of Pennsylvania, PA, USA for providing the *E. coli* LJ14 and MRE600 strains, and the proteomic platform of the Institute of Biophysics, Chinese Academy of Sciences, for mass spectra measurements of *Tte*RRF and its mutants, and Dr. Fuquan Yang for his suggestions on the revision of this manuscript.

References

[1] D.V. Freistroffer, M.Y. Pavlov, J. MacDougall, R.H. Buckingham, M. Ehrenberg, EMBO J. 16 (1997) 4126–4133.
[2] A.V. Zavialov, R.H. Buckingham, M. Ehrenberg, Cell 107 (2001) 115–124.
[3] A.V. Zavialov, L. Mora, R.H. Buckingham, M. Ehrenberg, Mol. Cell 10 (2002) 789–798.
[4] G. Grentzmann, P.J. Kelly, S. Laalami, M. Shuda, M.A. Firpo, Y. Cenatiempo, A. Kaji, RNA 4 (1998) 973–983.
[5] G. Hirokawa, N. Demeshkina, N. Iwakura, H. Kaji, Trends Biochem. Sci. 31 (2006) 143–149.
[6] L. Janosi, S. Mottagui-Tabar, L.A. Isaksson, Y. Sekine, E. Ohtsubo, S. Zhang, S. Goon, S. Nelken, M. Shuda, A. Kaji, EMBO J. 17 (1998) 1141–1151.
[7] T. Fujiwara, K. Ito, T. Nakayashiki, Y. Nakamura, FEBS Lett. 447 (1999) 297–302.
[8] L. Janosi, H. Hara, S. Zhang, A. Kaji, Adv. Biophys. 32 (1996) 121–201.
[9] L. Janosi, R. Ricker, A. Kaji, Biochimie 78 (1996) 959–969.
[10] M.Y. Pavlov, D. Freistroffer, J. MacDougall, R.H. Buckingham, M. Ehrenberg, EMBO J. 16 (1997) 4134–4141.
[11] R. Karimi, M.Y. Pavlov, R.H. Buckingham, M. Ehrenberg, Mol. Cell 3 (1999) 601–609.
[12] T. Kanai, S. Takeshita, H. Atomi, K. Umemura, M. Ueda, A. Tanaka, Eur. J. Biochem. 256 (1998) 212–220.
[13] N. Rolland, L. Janosi, M.A. Block, A. Shuda, E. Teyssier, C. Miege, C. Cheniclet, J. Carde, A. Kaji, J. Joyard, Proc. Natl. Acad. Sci. USA 96 (1999) 5464–5469.
[14] E. Teyssier, G. Hirokawa, A. Tretiakova, B. Jameson, A. Kaji, H. Kaji, Nucleic Acids Res. 31 (2003) 4218–4226.
[15] T. Toyoda, O.F. Tin, K. Ito, T. Fujiwara, T. Kumasaka, M. Yamamoto, M.B. Garber, Y. Nakamura, RNA 6 (2000) 1432–1444.
[16] H. Nakano, T. Yoshida, S. Uchiyama, M. Kawachi, H. Matsuo, T. Kato, A. Ohshima, Y. Yamaichi, T. Honda, H. Kato, Y. Yamagata, T. Ohkubo, Y. Kobayashi, J. Biol. Chem. 278 (2003) 3427–3436.
[17] M. Selmer, S. Al-Karadaghi, G. Hirokawa, A. Kaji, A. Liljas, Science 286 (1999) 2349–2352.
[18] K.K. Kim, K. Min, S.W. Suh, EMBO J. 19 (2000) 2362–2370.
[19] H. Nakano, S. Uchiyama, T. Yoshida, T. Ohkubo, H. Kato, Y. Yamagata, Y. Kobayashi, Acta Crystallogr. D Biol. 58 (2002) 124–126.
[20] T. Yoshida, S. Uchiyama, H. Nakano, H. Kashimori, H. Kijima, T. Ohshima, Y. Saihara, T. Ishino, H. Shimahara, T. Yoshida, K. Yokose, T. Ohkubo, A. Kaji, Y. Kobayashi, Biochemistry 40 (2001) 2387–2396.
[21] K. Saikrishnan, S.K. Kalapala, U. Varshney, M. Vijayan, J. Mol. Biol. 345 (2005) 29–38.
[22] P. Guo, L.Q. Zhang, H.J. Zhang, Y. Feng, G.Z. Jing, Biochem. J. 393 (2006) 767–777.
[23] A.R. Rao, U. Varshney, Microbiology 148 (2002) 3913–3920.
[24] P. Guo, L.Q. Zhang, Z. Qi, R.S. Chen, G.Z. Jing, J. Biochem. (Tokyo) 138 (2005) 89–94.
[25] X.L. Zhang, P. Guo, G.Z. Jing, Biotech. Lett. 25 (2003) 755–760.
[26] Y.M. Feng, Y.Y. Zhang, G.Z. Jing, Protein Expr. Purif. 25 (2002) 323–329.
[27] C.N. Pace, F. Vajdos, L. Fee, G. Grimsley, T. Gray, Protein Sci. 4 (1995) 2411–2423.
[28] M.M. Santoro, D.W. Bolen, Biochemistry 27 (1988) 8063–8068.
[29] S. Huang, X. Zou, P. Guo, L. Zhong, J. Peng, G.Z. Jing, Arch. Biochem. Biophys. 434 (2005) 86–92.
[30] L. Janosi, I. Shimizu, A. Kaji, Proc. Natl. Acad. Sci. USA 91 (1994) 4249–4253.
[31] Y.V. Griko, A. Gittis, E.E. Lattman, P.L. Privalov, J. Mol. Biol. 243 (1994) 93–99.
[32] H.J. Zhang, S. Huang, Y.M. Feng, P. Guo, G.Z. Jing, Arch. Biochem. Biophys. 441 (2005) 123–131.
[33] P.J. Gans, P.C. Lyu, M.C. Manning, R.W. Woody, N.R. Kallenbach, Biopolymers 31 (1991) 1605–1614.
[34] Y. Wang, D. Shortle, Fold Des. 2 (1997) 93–100.
[35] L.Q. Zhang, P. Guo, H.J. Zhang, G.Z. Jing, Arch. Biochem. Biophys. 450 (2006) 191–202.
[36] H.J. Zhang, X.R. Sheng, W.D. Niu, X.M. Pan, J.M. Zhou, J. Biol. Chem. 273 (1998) 7448–7456.
[37] Y. Han, X. Li, X.M. Pan, FEBS Lett. 528 (2002) 161–165.
[38] H.J. Zhang, X.R. Sheng, X.M. Pan, J.M. Zhou, Biochem. Biophys. Res. Commun. 238 (1997) 382–386.
[39] X.R. Sheng, H.J. Zhang, X.M. Pan, X. Li, J.M. Zhou, FEBS Lett. 413 (1997) 429–432.
[40] Y.H. Pang, X.Z. Li, S.B. Qin, H.J. Zhang, J.W. Chen, Int. J. Biochem. Biophys. 43 (2006) 351–359.
[41] M. Vihinen, Protein Eng. 1 (1987) 477–480.
[42] J.K. Myers, C.N. Pace, J.M. Scholtz, Protein Sci. 4 (1995) 2138–2148.